Title	Removal of iodide from water by chlorination and subsequent adsorption on powdered activated carbon
Author(s)	Ikari, Mariya; Matsui, Yoshihiko; Suzuki, Yuta et al.
Citation	Water research, 68, 227-237 https://doi.org/10.1016/j.watres.2014.10.021
Issue Date	2015-01-01
Doc URL	https://hdl.handle.net/2115/58012
Type	journal article
File Information	HUSCAP iodine.pdf

Removal of iodide from water by chlorination and subsequent adsorption on powdered activated carbon

Mariya Ikari[1], Yoshihiko Matsui[2,*], Yuta Suzuki[1], Taku Matsushita[2], and Nobutaka Shirasaki[2]

1 Graduate School of Engineering, Hokkaido University, N13W8, Sapporo 060-8628, Japan

2 Faculty of Engineering, Hokkaido University, N13W8, Sapporo 060-8628, Japan

* Corresponding author. Phone & Fax: +81-11-706-7280; e-mail: matsui@eng.hokudai.ac.jp

Abstract

Chlorine oxidation followed by treatment with activated carbon was studied as a possible method for removing radioactive iodine from water. Chlorination time, chlorine dose, the presence of natural organic matter (NOM), the presence of bromide ion (Br^-), and carbon particle size strongly affected iodine removal. Treatment with superfine powdered activated carbon (SPAC) after 10-min oxidation with chlorine (1 mg-Cl_2/L) removed 90% of the iodine in NOM-containing water (dissolved organic carbon concentration, 1.5 mg-C/L). Iodine removal in NOM-containing water increased with increasing chlorine dose up to 0.1 mg-Cl_2/L but decreased at chlorine doses of >1.0 mg-Cl_2/L. At a low chlorine dose, nonadsorbable iodide ion (I^-) was oxidized to adsorbable hypoiodous acid (HOI). When the chlorine dose was increased, some of the HOI reacted with NOM to form adsorbable organic iodine (organic-I). Increasing the chlorine dose further did not enhance iodine removal, owing to the formation of nonadsorbable iodate ion (IO_3^-). Co-existing Br^- depressed iodine removal, particularly in NOM-free water, because hypobromous acid (HOBr) formed and catalyzed the oxidation of HOI to IO_3^-. However, the effect of Br^- was small in the NOM-containing water because organic-I formed instead of IO_3^-. SPAC (median particle diameter, 0.62 μm) had a higher equilibrium adsorption capacity for organic-I than did conventional PAC (median diameter, 18.9 μm), but the capacities of PAC and SPAC for HOI were similar. The reason for the higher equilibrium adsorption capacity for organic-I was that organic-I was adsorbed principally on the exterior of the PAC particles and not inside the PAC particles, as indicated by direct visualization of the solid-phase iodine concentration profiles in PAC particles by field emission electron probe microanalysis. In contrast, HOI was adsorbed evenly throughout the entire PAC particle.

Keywords

iodide; iodate; SPAC; PAC; NOM

1. Introduction

The Tohoku Earthquake on 11 March 2011 resulted in the release of large amounts of radioactive materials including iodine-131 (^{131}I) into the environment from the Fukushima Daiichi nuclear power plant. After the accident, ^{131}I was detected in drinking water in 15 out of the total 47 prefectures in Japan: the highest concentration in a village of Fukushima Prefecture was 1000 Bq/kg-water and the highest concentration in Tokyo Metropolitan was 200 Bq/kg-water (Ikemoto and Magara 2011), which points to the importance of technologies for removal of radioactive substances during water purification processes. The radioactive iodine index levels for the restriction on drinking water intake in emergency by the Nuclear Safety Commission of Japan was 300 Bq/kg for the general public and 100 Bq/kg for infants (babies who take breast feeding or formula milk). The removal of radioactive iodine by 50–90 % was required.

The addition of powdered activated carbon (PAC) may be a feasible method for removal during conventional water treatment when accidents or incidents give rise to high levels of contamination in drinking water sources (Brown et al. 2008, Lettinga 1972). However, the efficacy of ^{131}I removal by PAC was not sufficiently high. Kosaka et al. (2012) surveyed ^{131}I removal in water purification plants after the Fukushima accident and found that the removal percentages achieved by granular activated carbon and PAC were merely 30–40% or less. The authors also conducted laboratory tests and attained the removal efficiencies of 60–70% by PAC of the dosage 50 mg/L and the contact time 30 minutes after chlorination of the dosage 0.5–1 mg-Cl_2/L and reaction time 10 minutes.

Dissolved I (including ^{131}I) exists in various forms: molecular iodine (I_2), hypoiodite ion (IO^-), hypoiodous acid (HOI), iodide ion (I^-), iodate ion (IO_3^-), and organic iodine (organic-I). At neutral pH iodine can be present in the latter four forms (Bichsel and von Gunten 2000a, Lettinga 1972), while iodine is commonly found as I^-, IO_3^-, and organic-I in environmental waters (Davis et al. 2009, Gong and Zhang 2013, Hansen et al. 2011). It has been reported that $^{131}I^-$ is poorly adsorbed by activated carbon (Ikeda and Tanaka 1975, Lettinga 1972). HOI is adsorbed on activated carbon to a greater extent than I^-: the adsorptive property of HOI is utilized in the iodine number, one of the most fundamental indicator widely used to characterize activated carbon as an adsorbent (AWWA 1974). The removal of HOI is due to adsorption while that of chlorine is reductive reaction. Because HOI is formed by oxidation of I^-, the combination of chlorination and PAC adsorption could be effective for $^{131}I^-$ removal (Lettinga 1972). However, $^{131}IO_3^-$, which is formed by oxidation of $HO^{131}I$, is reportedly not adsorbed by carbon (Lettinga 1972). Therefore, chlorination of $^{131}I^-$ at a high chlorine dose, a long reaction time, or both would reduce the extent of adsorptive removal compared to that at a low dose and a short reaction time. During aqueous oxidation in the presence of natural organic matter (NOM), HOI reacts with NOM to form iodo-organic byproducts (Bichsel and von Gunten 1999), which can be adsorbed by activated carbon (Summers et al. 1989). No systematic experimental study has been conducted to clarify how chlorination time, carbon type, and carbon dose affect iodine species distribution and, thus, iodine removal efficacy.

In this study, we systematically investigated the formation of iodine species by chlorination and their removal from water by activated carbon adsorption. The effects of chlorine dose, chlorination time, carbon particle size, NOM content, and co-existing bromide on iodine removal were evaluated to determine the optimum conditions for removal of radioactive iodine from water. We used ^{127}I rather than ^{131}I. But the adsorption behavior of ^{127}I is similar to that of ^{131}I. Therefore, information regarding ^{127}I removal can be expected to provide important insights for the removal of ^{131}I. The removal of iodide in water is also of great significance for controlling the formation of iodinated disinfection byproducts (Ding and Zhang 2009, Plewa et al. 2004). Hereafter, we refer to ^{127}I simply as I (or iodine).

2. Materials and methods

2.1. Sample water

NOM-free water was prepared by adding inorganic ions to ultrapure water (Milli-Q Advantage, Millipore) so that the ionic composition was equal to that of water from Lake Hakucho, Hokkaido, Japan (Table S1, Supplementary Material) (Ando et al. 2010). NOM water was prepared by adding Suwannee River NOM (International Humic Substance Society) to the NOM-free water to bring the dissolved organic carbon (DOC) concentration to 1.5 mg-C/L unless otherwise noted. Potassium iodide was added to the NOM-free water and the NOM water, and then the pH was adjusted to 7.0 with HCl or NaOH; the iodine concentration was 10 μg-I/L, which is typical of natural surface waters. In the experiments on iodine removal in the presence of bromide ion (Br^-), KBr was also added, at concentrations ranging from 0 to 2000 μg-Br/L (Jones et al. 2011, Richardson et al. 2008). All chemicals used were regent grade (Wako Pure Chemical, Osaka, Japan).

2.2. Activated carbon

Two types of activated carbon were used. A commercially available, thermally activated wood-based PAC (median particle diameter, 18.9 μm) was obtained from Taiko-W, Futamura Chemical (Nagoya, Japan). A superfine PAC (SPAC, median particle diameter, 0.62 μm; Figures S1 and S2, Supplementary Material) was prepared by microgrinding the PAC with a bead mill (Metawater, Tokyo) (Ando et al. 2010). PAC and SPAC were stored as slurries in ultrapure water at 4 °C and used after dilution. The particle size distributions of PAC and SPAC were determined with a laser-light scattering instrument (Microtrac MT3300EXII, Nikkiso, Tokyo) following the addition of a dispersant (Triton X-100, Kanto Chemical, Tokyo; final concentration, 0.08 vol%) and ultrasonication.

2.3. Batch oxidation and adsorption tests

Sample water was treated with chlorine (in the form of sodium hypochlorite, Wako Pure Chemical) at concentrations of 0.01–50 mg-Cl_2/L for 1–60 min, and then activated carbon was added. After a carbon contact time of up to 30 min, the suspension was filtered through a 0.2-μm membrane filter (DISMIC-25HP; Toyo Roshi Kaisha, Tokyo). In some experiments, water was treated first with carbon and then with chlorine. All experiments were conducted in the room temperature of 20 °C. Individual operation condition is described in figures. The concentration of free chlorine was determined by means of the *N*,*N*-diethyl-*p*-phenylenediamine colorimetric method (DR/4000U, Hach).

2.4. Iodine fractionation

The total iodine concentrations in sample waters were determined by means of inductively coupled plasma mass spectrometry (ICP-MS; 7700 series, Agilent Technologies) with tellurium as an internal standard (detection limit: 0.2 μg-I/L). Iodine fractionation was conducted by using total organic halide (TOX) analysis and ion-chromatography with post-column (IC-PC) derivatization (ICS-1100, PCM 520, UVD-510, Dionex) both for the samples treated with and without chlorine (Figures S3, Supplementary Material). The IC-PC was conducted according to the Dionex manual. KaBr/$NaNO_2$ mixture was used as PC derivatization reagent in order to form tri-iodide, which is detected using UV detector at 268 nm (detection limit: 0.1 μg-I/L).

Water samples with/without 10-min chlorination were treated with SPAC at a concentration of 100 mg/L for 30 min (these condition were determined for the complete removal of adsorbable iodine and bromine) and then filtered through a 0.2-μm PTFE membrane filter to obtain Sample A, which contained I^- and IO_3^- but did not contain HOI, as indicated by the results of a preliminary experiment (Supplementary Material, Section 1 and Figure S4). The total iodine concentration in Sample A was determined by ICP-MS, the IO_3^- concentration was determined for Sample A by IC-PC, and the I^- concentration was calculated for Sample A by subtracting the IO_3^- concentration from the total iodine concentration.

The organic-I concentrations were measured by means of TOX analysis, as follows (see Supplementary Material, Section 2 for details). After chlorination, NOM water was applied to a column of activated carbon. Then the column was washed with KNO_3 solution to remove any HOI bound to the carbon. The carbon packing was then removed from the column and heated in a muffle furnace, and the combustion gas was bubbled through Milli-Q water (the resulting solution was designated as Sample B). Any iodine in Sample B was regarded as organic-I (Tate et al. 1986). The iodine concentration in Sample B was determined by means of ICP-MS. The concentration of HOI was calculated by subtracting the iodine concentrations in Samples A and B from the initial iodine concentration, which was determined by ICP-MS. The percentages obtained by the fractionation method were verified by comparing them with the concentrations obtained by an alternative method (Supplementary Material, Section 3 and Figure S5) in which the concentration of HOI in the eluent from the activated carbon column used for TOX analysis was determined by ICP-MS.

2.5. Bromine fractionation

Bromine was fractionated in conjunction with iodine fractionation. The total bromine concentration and the bromate ion ($BrO_3^−$) concentration were determined by ICP-MS (detection limit: 5 μg-Br/L) and IC-PC (detection limit: 0.5 μg-Br/L), respectively (Figures S6, Supplementary Material). Because $Br^−$ is not adsorbed by activated carbon whereas hypobromous acid (HOBr), $BrO_3^−$, and organic bromine (organic-Br) are adsorbed (Siddiqui et al. 1996), the concentration of $Br^−$ was determined by means of ICP-MS for Sample A (the mechanism that HOBr is adsorbed but not reduced to $Br^−$ by activated carbon was confirmed by the decrease of total bromine concentration determined by ICP-MS. Section 3.3). The organic-Br concentration was measured for Sample B by means of ICP-MS. The HOBr concentration was calculated by subtracting the sum of the concentrations of $Br^−$, $BrO_3^−$, and organic-Br from the total bromine concentration.

2.6. Direct observation of iodine adsorbed on PAC particles

To obtain PAC particles containing adsorbed HOI and adsorbed organic-I, we conducted batch adsorption experiments. After batch adsorption, PAC particles were removed, placed on a silicon wafer, and then cut. Iodine adsorbed on the cut PAC particles was directly observed by means of scanning electron microscopy and field emission electron probe microanalysis (FE-EPMA; JXA-8530F, JEOL). Details of these experiments are described in the Supplementary Material (Section 4 and Figures S7 and S8).

3. Results and discussion

3.1. Iodine removal by activated carbon after chlorination

Without prior chlorination, I^- in the NOM-free water was not removed by activated carbon treatment (Figure S9, Supplementary Material). No removal of I^- from NOM water was observed either. In contrast, when chlorine was added to the NOM-free water before activated carbon treatment, about 40% of the iodine was removed. After the chlorination, iodine in the NOM water was removed at a higher percentage (90%) by activated carbon treatment than in the NOM-free water. This removal percentage was similar but slightly higher than the DOC removal percentage (80%). The similar removal suggests that the formation of organic-I was responsible for the high iodine removal percentage in the presence of NOM. The slightly higher removal is possibly due to HOI removal.

We further studied the effect of NOM by varying the initial DOC concentration in the sample water. Even a DOC concentration as low as 0.5 mg-C/L drastically improved adsorptive removal of iodine by SPAC after chlorination (Panel A of Figure 1). At a fixed SPAC dose of 100 mg/L, the residual iodine ratio decreased as the initial DOC concentration was increased from 0 to 3 mg-C/L, but the ratio increased as the DOC concentration was increased further from 3 to 10 mg-C/L. This increase in residual ratio was due to the insufficiency of the carbon dose; when the carbon dose was increased to >100 mg/L, the ratio continued to decrease with increasing DOC concentration above 3 mg-C/L (Figure 1, Panel A, dashed line). The residual ratios indicated by the triangles in Panel A of Figure 1 were achieved when a sufficient amount of SPAC was used; the amount that was sufficient was confirmed by testing various combinations of SPAC dose and DOC concentration (Figure 1, Panel B). The data points indicated by the triangles can be considered to be the lowest residual iodine ratios attainable by adsorptive removal with SPAC. These results indicate that the percentage of iodine converted to adsorbable forms increased with increasing NOM concentration: at the DOC of 10 mg-C/L, 95 % of I^- was converted to adsorbable forms.

3.2. Chlorine-dose dependence and iodine fractionation analysis

The results described in the previous section indicate that the iodine was converted to an adsorbable form by chlorination. Next we studied the effect of chlorine dose. For NOM-free water, a chlorine dose of approximately 0.1 mg-Cl_2/L was found to be optimal, yielding the lowest residual iodine ratio (Figure S10, Supplementary Material). A similar trend was observed for NOM water, although low residual iodine ratios were observed over a broader range of chlorine doses (0.1–1.0 mg-Cl_2/L). Iodine removal increased with increasing chlorine dose up to 0.1 mg-Cl_2/L but decreased at chlorine doses of >1.0 mg-Cl_2/L. Overall, the residual ratios were lower in the presence of NOM than in its absence.

To elucidate the mechanism of the dependence of iodine removal on chlorine dose, we conducted iodine fractionation. In NOM-free water (Figure 2, Panel A), the production of HOI was highest at a chlorine dose of 0.05–0.1 mg-Cl_2/L, and production decreased as the chlorine dose was increased from 0.1 to 10 mg-Cl_2/L. Therefore, a moderate chlorine dose (0.05–0.1 mg-Cl_2/L) was most effective for the formation of HOI, which was adsorbed by activated carbon. At high chlorine doses (>0.1 mg-Cl_2/L), IO_3^- formed, and IO_3^- became the major species at chlorine doses of >1 mg-Cl_2/L. The percentages of IO_3^- fraction were almost similar but somewhat higher than those calculated by the reaction rate constants reported previously (Bichsel and von Gunten 1999): the experimental percentages were 1.9, 38, and 100 while the calculated ones were 1.5, 14, and 88 at the chlorine doses of 0.1, 1 and 10 mg-Cl_2/L, respectively. The somewhat higher IO_3^- percentages might be due to the enhanced oxidation at very low iodine concentration in our experiments.

When the water contained NOM (DOC concentration, 1.5 mg-C/L), organic-I formed (Figure 2, Panel B). The concentration of organic-I increased as the chlorine dose was increased from 0.05 to 1 mg-Cl_2/L, and then it decreased. The latter finding is qualitatively in agreement with the results of studies of iodotrihalomethane formation, in which an increase in chlorine doses was found to lead to a decrease in the levels of iodinated organic byproducts and an increase in IO_3^- formation (Bichsel and von Gunten 2000b, Hua et al. 2006). We found that organic-I was the major species at high chlorine doses (0.5–5 mg-Cl_2/L) and that HOI was the major species at low doses (0.05–0.5 mg-Cl_2/L). We inferred that at chlorine doses of >1.0 mg-Cl_2/L in the NOM-free water, HOI was promptly oxidized to IO_3^-, which was not adsorbed by activated carbon. However, in the NOM water at a high chlorine dose, the formation of organic-I prevented the formation of IO_3^-. The use of chlorine doses of 0.1–0.5 mg-Cl_2/L resulted in the formation of the highest amount of adsorbable iodine (HOI and organic-I) and thus to the highest iodine removal efficiency.

3.3. Effect of co-existing Br^- on the removal of I^-

Br^- have been shown to influence the formation of iodinated trihalomethane during water treatment by means of chlorination (Jones et al. 2012), and thus the presence of Br^- can be expected to have an impact on iodine oxidation by chlorination. As shown in Panel A of Figure 3, the residual iodine ratio in the NOM-free water slightly increased as the Br^- concentration was increased from 0 to 10 μg-Br/L, and the increase in residual iodine ratio with increasing Br^- concentration was more rapid in the concentration range from 10 to 200 μg-Br/L. This result indicates that co-existing Br^- in the water inhibited iodine removal. In the NOM-free water, IO_3^- formation increased dramatically with increasing initial Br^- concentration in the range from 10 to 200 μg/L (Panel B of Figure 3). In contrast, little IO_3^- was formed in the presence of Br^- in the NOM water. The effect of Br^- on iodine removal was largely attributable to enhanced formation of nonadsorbable IO_3^- in the presence of Br^-.

To further elucidate the effect of Br^- on the oxidation of I^- by chlorine, we conducted iodine and bromine fractionation. As shown in Panel A1 of Figure 4, in NOM-free water containing Br^-, the proportion of HOI was the largest at a chlorine dose of 0.1 mg-Cl_2/L. IO_3^- formed at chlorine doses of >0.1 mg-Cl_2/L and became the major iodine species at chlorine doses of >1 mg-Cl_2/L. This result was similar to that observed in the absence of Br^- (Figure 2, Panel A). However, the percentage of IO_3^- formation at chlorine doses of >0.1 mg-Cl_2/L (and particularly at a chlorine dose of ~1 mg-Cl_2/L) was higher in the presence of Br^- than in the absence of Br^-. At a chlorine dose of 1 mg-Cl_2/L, IO_3^- formation in the presence of Br^- was 1.7 times that in the absence of Br^-. Bromine fractionation revealed that in the NOM-free water, HOBr was formed at a chlorine dose of 0.05 mg-Cl_2/L, and the proportion of HOBr increased with increasing chlorine dose up to 2 mg-Cl_2/L (Figure 4, Panel B1). This chlorine dose range roughly coincided with the range at which IO_3^- formation was higher in the presence of Br^- than in its absence. It was recently reported that increasing the Br^- concentration increases the oxidation of HOI to IO_3^- (Criquet et al. 2012), as a result of a bromide-catalyzed process where the following reaction sequence is proposed. HOBr is formed through the reaction of chlorine with Br^-. HOBr then oxidizes HOI to IO_3^- and thereby HOBr is reduced to Br^-. Our results confirm that Br^-/HOBr-catalyzed process: we found that when HOBr was formed by the oxidation of Br^- by chlorine, the oxidation of HOI to IO_3^- was enhanced.

In the NOM water, iodine removal was not greatly influenced by the presence of Br^- (Panel A of Figure 3). However, the nature of the adsorbed iodine species differed in the absence and presence of Br^- (Figure 2, Panel B; Figure 4, Panel A2). More organic-I was formed at a chlorine dose of

~0.1 mg/L in the presence of Br^- than in its absence, while more IO_3^- was formed at chlorine doses > 5 mg/L. The enhanced formation of organic-I may possibly be due to a reaction process similar to the Br^-/HOBr-catalyzed process of IO_3^- formation. As shown in panel B2 of Figure 4, the proportion of HOBr was high at chlorine doses of >0.5 mg-Cl_2/L. However, at chlorine doses ranging from 0.05 to 0.1 mg-Cl_2/L, the proportion of HOBr was low. Nonetheless, a large amount of organic-I was formed at this low chlorine dose range. There is, however, a possibility that HOBr had been once formed but it was converted back to Br^-. Without clear data of HOBr formation, it cannot be concluded that organic-I was formed through the Br^-/HOBr-catalyzed process. Further study is granted for the mechanism of the enhanced formation of organic-I in the presence of bromide.

3.4. Effects of chlorination and reaction sequence

We also evaluated the effect of chlorination time (1–60 min) on the residual iodine ratio (Figure 5). The lowest residual ratio was observed at the shortest chlorination time (1 min). This result suggests that the oxidation of I^- to HOI was fast and that the oxidation of HOI to IO_3^- occurred continuously as long as free chlorine was present in the water. The fast oxidation reaction of I^- to HOI and the following slow oxidation reaction of HOI to IO_3^- are in agreement with the reaction kinetics calculations with the rate constants reported previously (Bichsel and von Gunten 1999, Criquet et al. 2012, Kumar et al. 1986): half life of I^- in the presence of HOCl of > 1mg-Cl_2/L is < 1 ms while that of HOI was < 45 min. Therefore chlorination in the presence of carbon could enhance iodine removal if HOI adsorption occurred before HOI was oxidized to IO_3^-. To evaluate this possibility, we conducted two experiments: in one experiment (Case 1), water was chlorinated first and then activated carbon was added, whereas in the other experiment (Case 2), water was chlorinated after activated carbon was added.

In the NOM-free water (Figure 6, panel A1), lower residual iodine ratios were obtained in Case 2 than in Case 1 at chlorine doses of >0.3 mg-Cl_2/L. Panel A2 of Figure 6 shows IO_3^- formation ratio and residual chlorine ratios for the two experiments. In Case 2, the formation of IO_3^- was depressed compared to that in Case 1. The carbon consumed the chlorine so that the formation of IO_3^- by oxidation of HOI was suppressed. Therefore, after HOI formed, it was efficiently adsorbed by the carbon. At low chlorine doses (<0.2 mg-Cl_2/L), however, iodine removal was lower in Case 2 than in Case 1, owing to the consumption of chlorine by carbon before the chlorine could oxidize I^- to HOI.

We also compared the results for Cases 1 and 2 with NOM water. Although iodine removal was higher in Case 2 than in Case 1 at high chlorine doses (>5 mg-Cl_2/L; Figure 6, panel B1), the difference between the two cases for the NOM water was not as clear as that for the NOM-free water. This result is reasonable because IO_3^- formation in the NOM water was depressed by the formation of organic-I, even in the absence of activated carbon; the IO_3^- formation was smaller in the presence of NOM than in the absence of NOM (compare Panels B2 and A2 of Figure 6). The formation of IO_3^- was also somewhat depressed when the water was treated with activated carbon prior to chlorination (Case 2), and consequently iodine removal was slightly higher in Case 2 than in Case 1.

In Case 1, increasing the chlorine contact time depressed adsorptive removal of iodine because of the formation of IO_3^- from HOI (Figure 5). However, a similar trend was not observed in Case 2, as shown in panels A1 and B1 of Figure 7. The residual iodine ratios did not increase with increasing chlorine contact time; instead, the removal percentage increased until 10 min. This result also supports the reaction mechanism described above: soon after I^- was oxidized to HOI by chlorine, the HOI was adsorbed by the carbon, and only some of the HOI was further oxidized to IO_3^- in the presence of carbon. Meanwhile, activated carbon consumed the chlorine, which disappeared after 10 min (Figure 7, panels A2 and B2). Therefore, iodine removal did not increase; rather, it reached a constant level after 10 min.

3.5. Effect of carbon particle size on adsorption capacity

The effect of carbon particle size on adsorption capacity was examined by calculating the adsorption isotherms from data obtained by batch adsorption experiments on prechlorinated sample water containing iodine. In the batch adsorption experiments, the water-phase iodine concentration did not change when the contact time was increased from 30 to 60 min (Figure S11, Supplementary Material). Therefore, we assumed that adsorption equilibrium was attained at a contact time of 30 min. The adsorption isotherms (Figure 8) were obtained by mass balance after contact with PAC or SPAC, but note that the iodine in the water-phase might have consisted of both adsorbable iodine (HOI and/or organic-I) and nonadsorbable iodine (I^- and IO_3^-). At a given water-phase iodine concentration (x-axis of Figure 8), which was attained by one removal percentage, the adsorbable iodine (HOI and/or organic-I) concentrations were the same between SPAC and PAC because the prechlorination conditions were the same for the water samples. Therefore, the adsorption capacities of PAC and SPAC can be compared at a given water-phase concentration in Figure 8. The adsorption isotherms for SPAC and PAC were the same for the NOM-free water (Figure 8, Panel A), whereas the isotherms were different for the NOM water (Figure 8, Panel B). In the presence of NOM, the adsorption capacity of PAC was roughly half that of SPAC. Such a trend of the lower adsorption capacity of PAC than of SPAC is reported for NOM adsorption (Ando et al. 2010), and the low adsorption capacity of PAC compared with that of SPAC is due to the difference in carbon particle size and to external adsorption: adsorbates do not diffuse into the interior of the PAC particles and instead are preferentially adsorbed near the particle surface (Ando et al. 2011, Matsui et al. 2011). Therefore, not all of the internal pore surface of the PAC particles is used for adsorption. In contrast, adsorbates can completely penetrate SPAC particles because the radial diffusion distance is short, and thus the entire internal pore surface of the SPAC particles is used for adsorption. The fact that there was no difference in adsorption capacity between PAC and SPAC for the NOM-free water indicates that internal adsorption occurred for both PAC and SPAC. Therefore, the experimental results for the NOM-free water indicate that HOI was adsorbed on the internal pore surface of the PAC particles. The experimental results for the NOM water indicate that organic-I was adsorbed on the external surface of the PAC particles. This is reasonable if the adsorption characteristics of organic-I (or iodinated NOM) are similar to those of the parent NOM, which exhibits external adsorption (Ando et al. 2010).

3.6. Visualization of solid-phase iodine concentration profiles

To verify the internal adsorption of HOI and the external adsorption of organic-I on PAC particles, we visualized the solid-phase iodine concentration profiles by using FE-EPMA. Panels A3 and A4 of Figure 9 are iodine intensity maps of a cut PAC particle containing adsorbed HOI formed by chlorination in the NOM-free water. The intensity from iodine was slightly lower outside the particle (~230 cps) than inside the particle (~270 cps). However, this difference may have been due to the edge effect: the intensity from carbon was also slightly lower outside than inside (Figure 9, Panel A2). An area of low intensity was also observed at the center right of the sample. However, there was a large open pore at the center right (Figure 9, Pane A1), and thus the low intensity at the center right does not indicate low iodine concentration. Therefore, this result suggests that HOI was adsorbed uniformly in the PAC particle.

Iodine intensity maps of a cut sample of a PAC particle containing adsorbed organic-I formed by chlorination in the NOM water are shown in panels B3 and B4 of Figure 9 (both HOI and organic-I were formed in the NOM water, but the HOI was eluted from the carbon particle, as described in the Supplementary Material, Section 3). For this particle, the iodine intensity was not higher inside than outside; instead the intensity was lower inside (~110 cps) than outside (~160 cps). Four open pores were observed in the sample (Figure 9, panel B1). Therefore, the low intensity in the area close to these pores may have been due to the pores. However, there was a large area of low intensity (the area surrounded by the dotted line in Figure 9) away from these pores. This result indicates that the concentration of solid-phase organic-I was lower inside the carbon particle than outside and that organic-I was adsorbed more on the outside than on the inside.

Overall, the visualization verified the hypothesis described in the previous section (external adsorption of organic-I and internal adsorption of HOI). The organic-I was adsorbed on the surface region of the PAC particles, but the total external surface area per unit weight of carbon was increased by the pulverization of PAC to SPAC. Accordingly, the increase in the surface area gave an advantage to SPAC compared to PAC with respect to organic-I adsorption capacity.

4. Conclusions

(1) HOI and organic-I were adsorbed by activated carbon. In the presence of NOM, HOI was the major adsorbed species at a low chlorine dose, whereas organic-I was the major species at a high chlorine dose.

(2) There was an optimum chlorine dose for transformation of iodine to its adsorbable forms. The optimum dose was relatively low: 0.5–1.0 mg-Cl_2/L for 10 μg/L of iodine in the presence of NOM (1.5 mg-DOC/L). A long chlorination time reduced iodine removal because of the transformation of

HOI to nonadsorbable IO_3^-. The optimum chlorination time was ~1 min or less.

(3) In the presence of Br^- in the NOM-free water, I^- was easily transformed into IO_3^- by chlorination even at low chlorine doses (0.1–0.2 mg-Cl_2/L), owing to a Br^-/HOBr-catalyzed process; and this process resulted in lower iodine removal in the presence of Br^- than in its absence. In the NOM water, however, co-existing Br^- did not decrease iodine removal greatly, owing to the high production of organic-I.

(4) In the NOM-free water, chlorination in the presence of PAC (Case 2) could enhance iodine removal compared with prechlorination followed by PAC adsorption (Case 1). This difference was due to the fact that in Case 2, the formation of IO_3^- was minimized by the consumption of chlorine by carbon. After HOI formed, it was readily adsorbed by the activated carbon before it could be oxidized to IO_3^-. In the NOM water, however, iodine removal was similar in Cases 1 and 2.

(5) The HOI adsorption capacity of SPAC was similar to that of PAC. For organic-I, however, SPAC showed higher adsorption capacity than PAC, because of the external adsorption (organic-I was adsorbed close to the PAC particle surface).

(6) FE-EPMA of PAC particles containing adsorbed HOI and organic-I revealed that the organic-I was adsorbed mostly close to the external surface of the PAC particles, whereas HOI was adsorbed uniformly in the PAC particles.

Acknowledgments

This study was supported by a Grant-in-Aid for Scientific Research S (no. 24226012) from the Japan Society for the Promotion of Science.

Appendix. Supplementary Information

Figure S1-S11 and Table S1 are available in the online version at ######.

References

Ando, N., Matsui, Y., Kurotobi, R., Nakano, Y., Matsushita, T. and Ohno, K. (2010) Comparison of natural organic matter adsorption capacities of super-powdered activated carbon and powdered activated Carbon. Water Research 44(14), 4127-4136.

Ando, N., Matsui, Y., Matsushita, T. and Ohno, K. (2011) Direct observation of solid-phase adsorbate concentration profile in powdered activated carbon particle to elucidate mechanism of high adsorption capacity on super-powdered activated carbon. Water Research 45(2), 761-767.

AWWA (1974) AWWA Standard for Granular Activated Carbon. Journal of American Water Works Association 66(11), 672-681.

Bichsel, Y. and von Gunten, U. (1999) Oxidation of iodide and hypoiodous acid in the disinfection of natural waters. Environmental Science & Technology 33(22), 4040-4045.

Bichsel, Y. and von Gunten, U. (2000a) Hypoiodous acid: kinetics of the buffer-catalyzed disproportionation. Water Research 34(12), 3197-3203.

Bichsel, Y. and von Gunten, U. (2000b) Formation of iodo-trihalomethanes during disinfection and oxidation of iodide-containing waters. Environmental Science & Technology 34(13), 2784-2791.

Brown, J., Hammond, D. and Wilkins, B.T., (2008) Handbook for Assessing the Impact of a Radiological Incident on Levels of Radioactivity in Drinking Water and Risks to Operatives at Water Treatment Works, Public Health England, http://www.hpa.org.uk/webc/HPAwebFile/HPAweb_C/1215762210590 (accessed on 23/7/2013).

Criquet, J., Allard, S., Salhi, E., Joll, C.A., Heitz, A. and von Gunten, U. (2012) Iodate and iodo-trihalomethane formation during chlorination of iodide-containing waters: role of bromide. Environmental Science & Technology 46(13), 7350-7357.

Davis, J.A., Fox, P.M. and Fuhrmann, M., (2009) Redox and Sorption Reactions of Iodine and Cesium During Transport Through Aquifer Sediments (NUREG/CR-6977), Unites States Nuclear

Regulatory Commission, http://www.nrc.gov/reading-rm/doc-collections/nuregs/contract/cr6977/ (accessed on 12/4/2014).

Ding, G. and Zhang, X. (2009) A Picture of Polar Iodinated Disinfection Byproducts in Drinking Water by (UPLC/)ESI-tqMS. Environmental Science & Technology 43(24), 9287-9293.

Gong, T. and Zhang, X. (2013) Determination of iodide, iodate and organo-iodine in waters with a new total organic iodine measurement approach. Water Research 47(17), 6660-6669.

Hansen, V., Yi, P., Hou, X., Aldahan, A., Roos, P. and Possnert, G. (2011) Iodide and iodate (129I and 127I) in surface water of the Baltic Sea, Kattegat and Skagerrak. Science of the Total Environment 412–413(0), 296-303.

Hua, G., Reckhow, D.A. and Kim, J. (2006) Effect of Bromide and Iodide Ions on the Formation and Speciation of Disinfection Byproducts during Chlorination. Environmental Science & Technology 40(9), 3050-3056.

Ikeda, N. and Tanaka, K. (1975) Column chromatographic separation of radioactive tellurate, tellurite, iodide and iodate by active charcoal. Journal of Chromatography A 114(2), 389-395.

Ikemoto, T. and Magara, Y. (2011) Measures against impacts of nuclear disaster on drinking water supply systems in Japan Water Practice and Technology 6.doi:10.2166/wpt.2011078.

Jones, D.B., Saglam, A., Triger, A., Song, H. and Karanfil, T. (2011) I-THM formation and speciation: preformed monochloramine versus prechlorination followed by ammonia addition. Environmental Science & Technology 45(24), 10429-10437.

Jones, D.B., Saglam, A., Song, H. and Karanfil, T. (2012) The impact of bromide/iodide concentration and ratio on iodinated trihalomethane formation and speciation. Water Research 46(1), 11-20.

Kosaka, K., Asami, M., Kobashigawa, N., Ohkubo, K., Terada, H., Kishida, N. and Akiba, M. (2012) Removal of radioactive iodine and cesium in water purification processes after an explosion at a nuclear power plant due to the Great East Japan Earthquake. Water Research 46(14), 4397-4404.

Kumar, K., Day, R.A. and Margerum, D.W. (1986) Atom-transfer redox kinetics: general-acid-assisted oxidation of iodide by chloramines and hypochlorite. Inorganic Chemistry 25(24), 4344-4350.

Lettinga, G. (1972) Radioactivity and Water Supplies. . 1972. , Delft, the Netherlands.

Matsui, Y., Ando, N., Yoshida, T., Kurotobi, R., Matsushita, T. and Ohno, K. (2011) Modeling high adsorption capacity and kinetics of organic macromolecules on super-powdered activated carbon. Water Research 45(4), 1720-1728.

Plewa, M.J., Wagner, E.D., Richardson, S.D., Thruston, A.D., Woo, Y.-T. and McKague, A.B. (2004) Chemical and Biological Characterization of Newly Discovered Iodoacid Drinking Water Disinfection Byproducts. Environmental Science & Technology 38(18), 4713-4722.

Richardson, S.D., Fasano, F., Ellington, J.J., Crumley, F.G., Buettner, K.M., Evans, J.J., Blount, B.C., Silva, L.K., Waite, T.J., Luther, G.W., McKague, A.B., Miltner, R.J., Wagner, E.D. and Plewa, M.J. (2008) Occurrence and Mammalian Cell Toxicity of Iodinated Disinfection Byproducts in Drinking Water. Environmental Science & Technology 42(22), 8330-8338.

Siddiqui, M., Zhai, W., Amy, G. and Mysore, C. (1996) Bromate ion removal by activated carbon. Water Research 30(7), 1651-1660.

Summers, R.S., Fuchs, F. and Sontheimer, H. (1989) The fate and removal of radioactive iodine in the aquatic environment,Aquatic Humic Substances: Influence on Fate and Treatment of Pollutants. MacCarthy, I.H.S.a.P. (ed), American Chemical Society, Advances in Chemistry Series, Number 219, Washington DC.

Tate, C.H., Chow, B.M., Clark, R.R., Grams, N.E. and Hashimoto, L.K., (1986) EPA Method Study 32: Method 450.1-Total Organic Halide (TOX), Environmental Monitoring and System Laboratory, USEPA, Cincinnati, Ohio, USA, http://www.epa.gov/nscep/index.html (accessed on 18/5/2014).

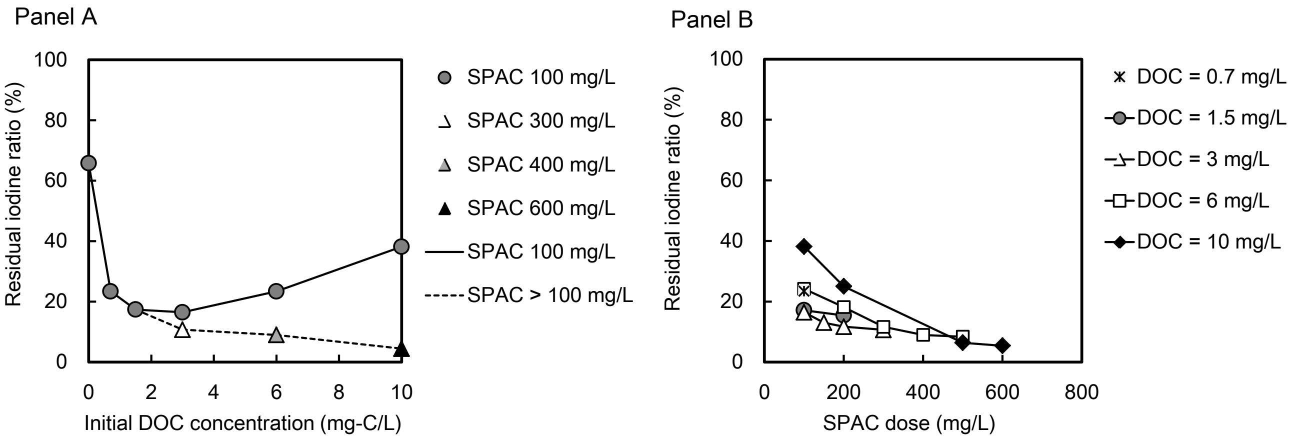

Figure 1. Effect of initial DOC concentration (left) and SPAC dose (right) on iodine removal from NOM water by chlorination followed by treatment with SPAC. Initial I^- concentration in sample water, 10 μg-I/L; chlorine dose, 1 mg-Cl_2/L; chlorination time, 10 min; carbon contact time, 30 min.

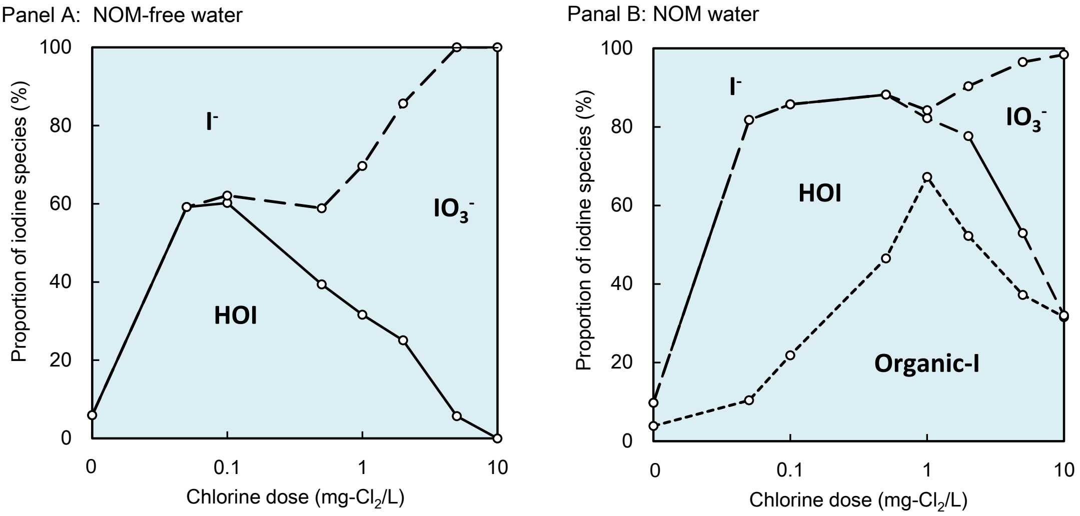

Figure 2. Proportions of iodine species in NOM-free water (left) and NOM water (right) as a function of chlorine dose. Chlorination time, 10 min; initial I$^-$ concentration in sample water, 10 μg-I/L; initial DOC concentration in NOM water, 1.5 mg-C/L.

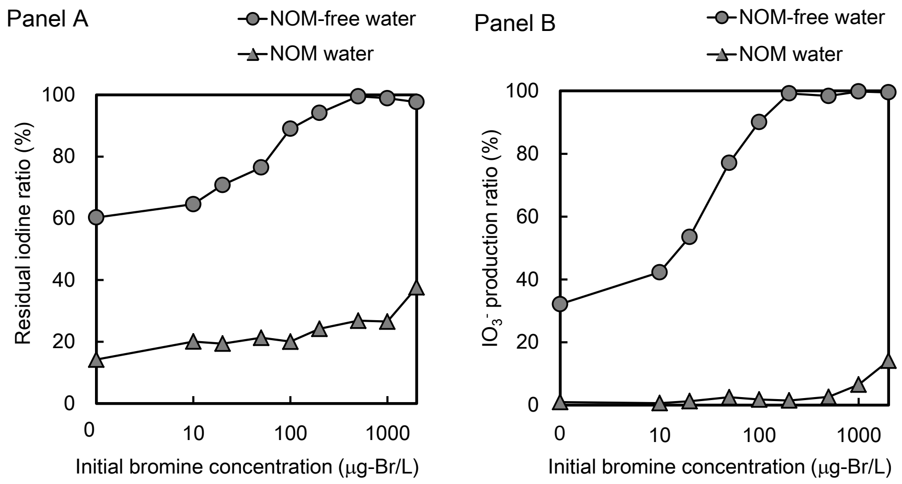

Figure 3. Effect of initial Br^- concentration on adsorptive removal of iodine (left) and IO_3^- production ratio (right). SPAC dose, 100 mg/L; initial I^- concentration in sample water, 10 μg-I/L; initial DOC concentration in NOM water, 1.5 mg-C/L; chlorine dose, 1.0 mg-Cl_2/L; chlorination time, 10 min; carbon contact time, 30 min.

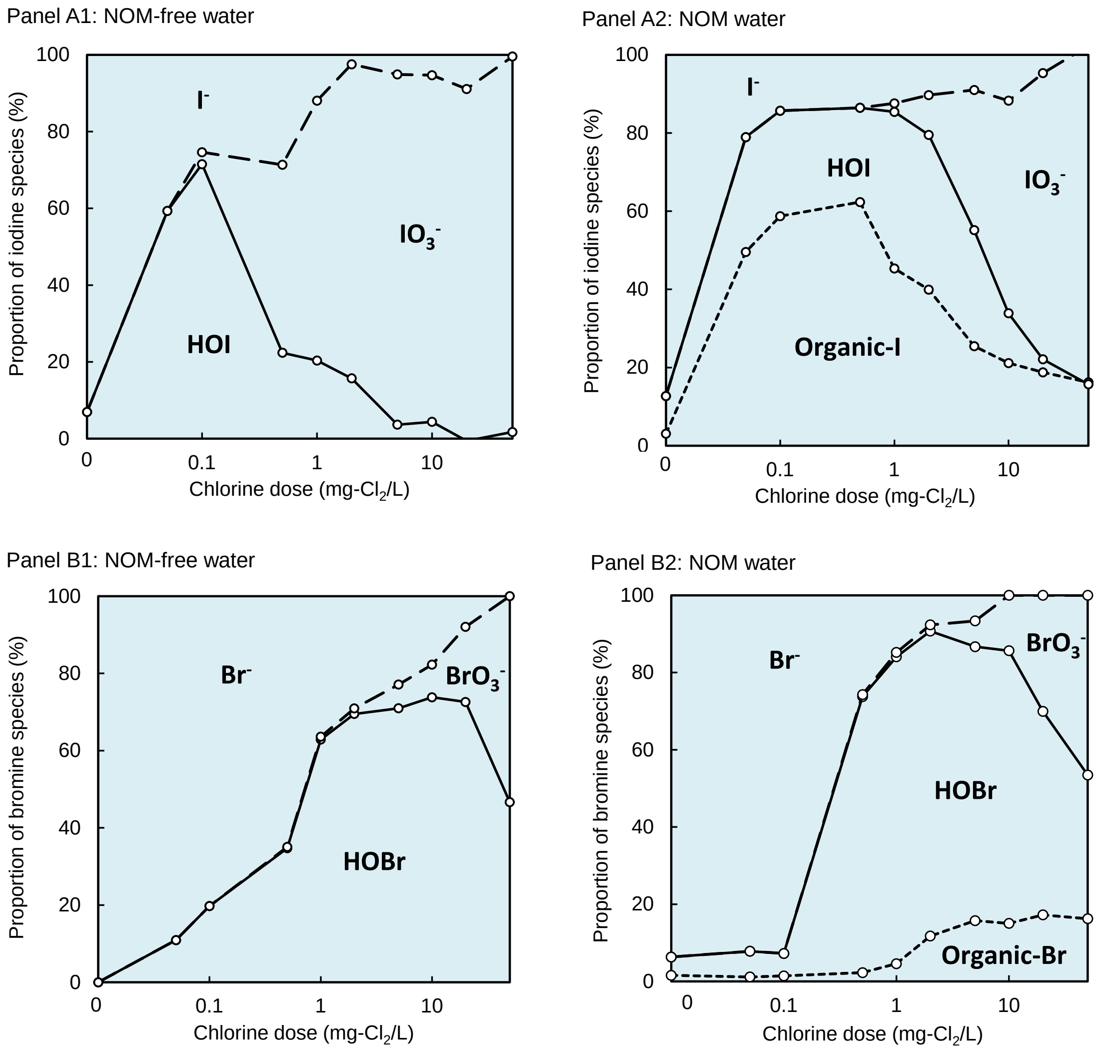

Panel A1: NOM-free water

Panel A2: NOM water

Panel B1: NOM-free water

Panel B2: NOM water

Figure 4. Proportions of iodine species (top) and bromine species (bottom) formed in the presence of Br$^-$ as a function of chlorine dose. Chlorination time, 10 min; initial I$^-$ concentration in sample water, 10 μg-I/L; initial Br$^-$ concentration, 100 μg-Br/L; initial DOC concentration in NOM water, 1.5 mg-C/L.

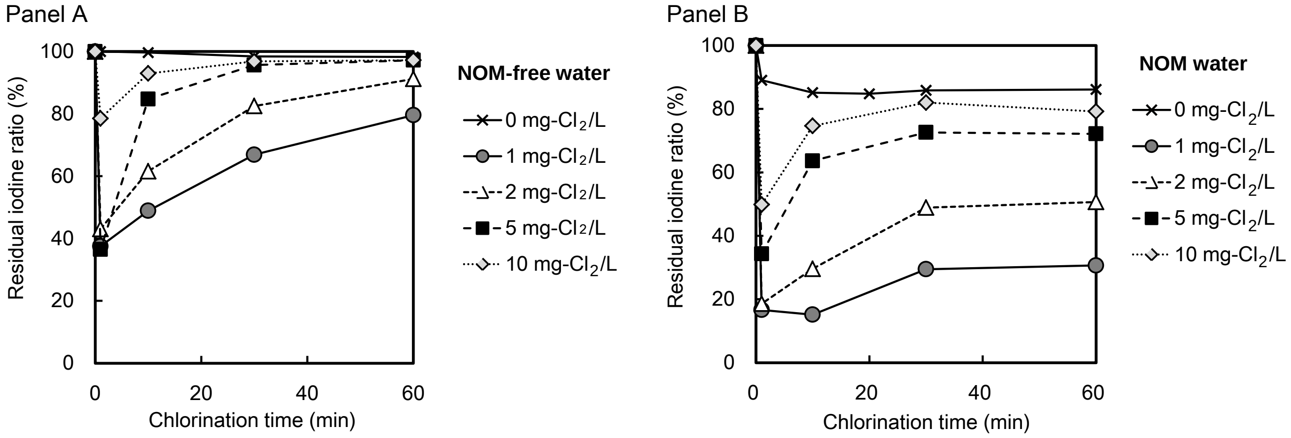

Figure 5. Effects of chlorination time and chlorine dose on iodine removal from NOM-free water (left) and NOM water (right). After chlorination, 100 mg/L of SPAC was added. Initial I^- concentration in sample water, 10 μg-I/L; initial DOC concentration in NOM water, 1.5 mg-C/L; carbon contact time, 30 min.

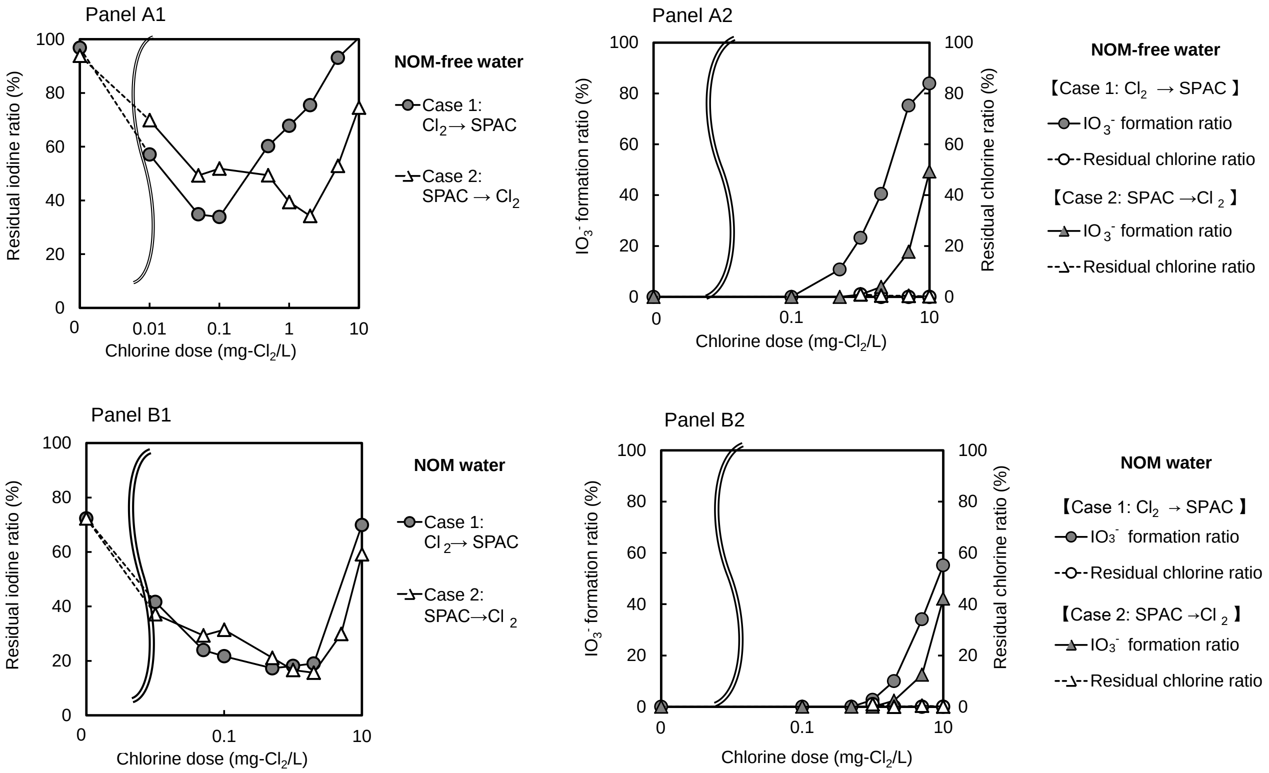

Figure 6. Effects of reaction sequence on residual iodine ratios (left) and IO_3^- formation ratios (right) in NOM-free water (top) and NOM water (bottom). Case 1: Chlorination followed by activated carbon treatment. Case 2: Chlorination preceded by activated carbon treatment. Initial I^- concentration in NOM water, 10 μg-I/L; SPAC dose, 100 mg/L; chlorination time, 10 min; carbon contact time for Case 1, 30 min; initial DOC concentration in NOM water, 1.5 mg-C/L.

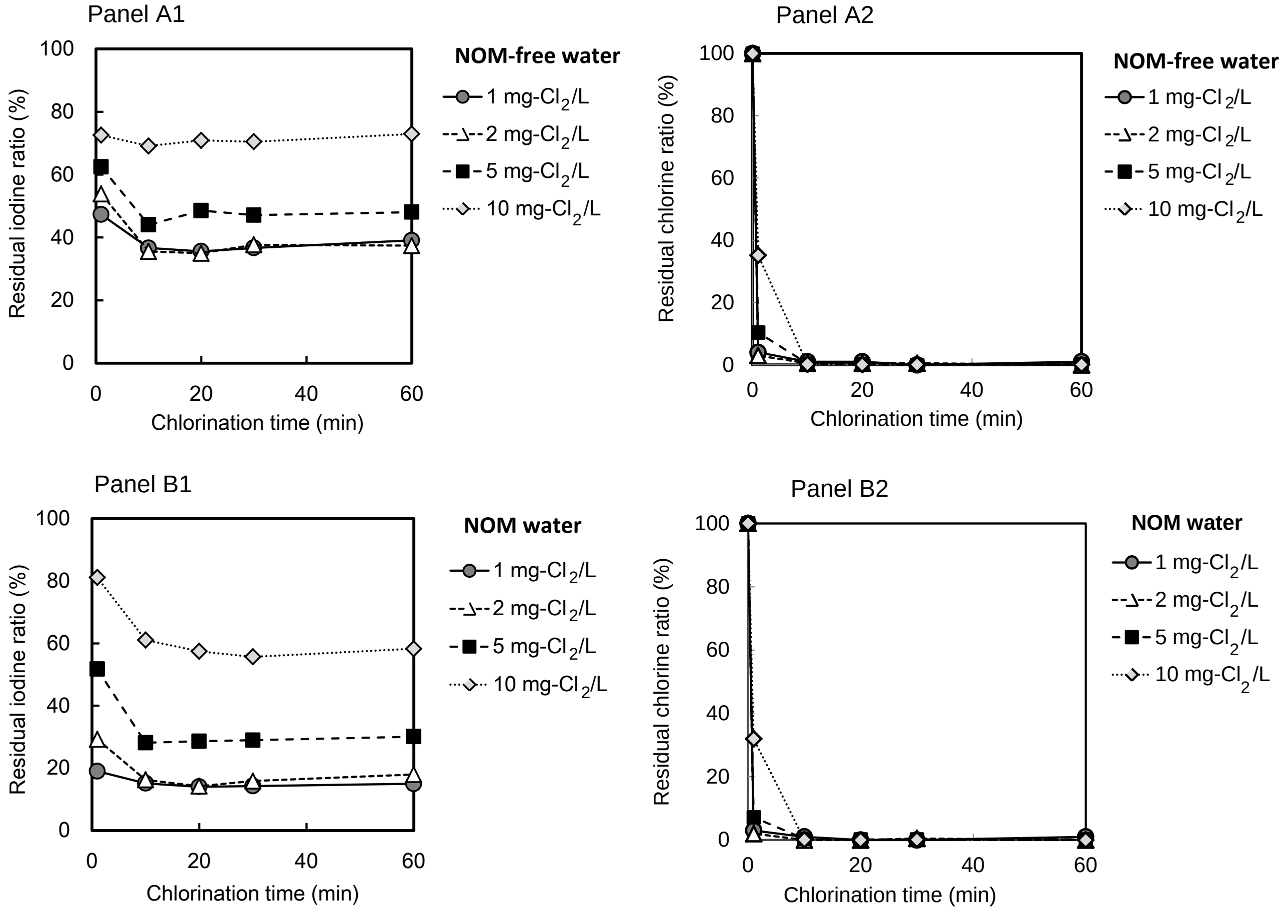

Figure 7. Effects of chlorination time and chlorine dose on residual iodine ratio (left) and residual chlorine ratio (right) in NOM-free water (top) and NOM water (bottom). After SPAC was added to the sample water, chlorine was added. SPAC dose, 100 mg/L; initial I$^-$ concentration in sample water, 10 μg-I/L; initial DOC concentration, 1.5 mg-C/L.

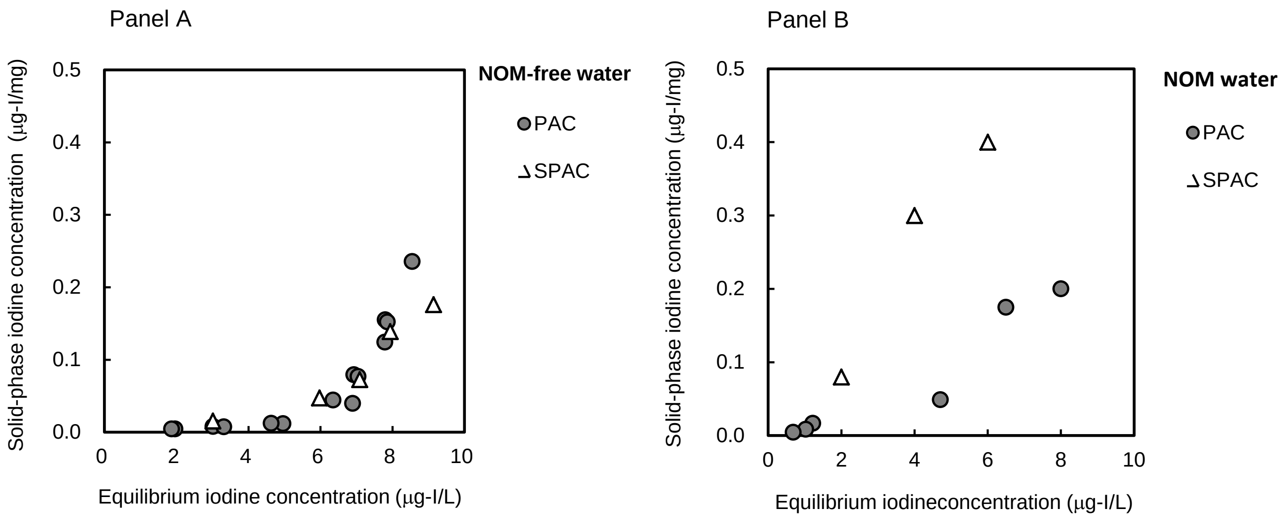

Figure 8. Comparison of iodine adsorption isotherms for PAC and SPAC in NOM-free water (left) and NOM water (right). After chlorination of sample water for 10 min, PAC or SPAC was added. Initial I^- concentration in sample water (NOM water and NOM-free water), 10 μg-I/L; chlorine doses, 0.5 mg-Cl_2/L for NOM-free water and 1.0 mg-Cl_2/L for NOM water; initial DOC concentration in NOM water, 1.5 mg-C/L; carbon contact time, 30 min.

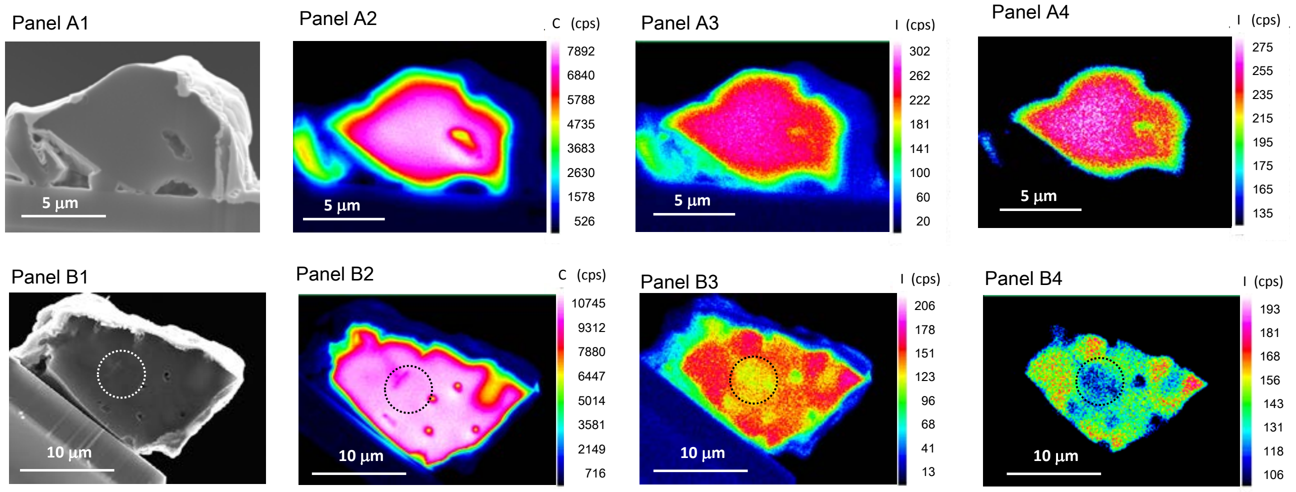

Figure 9. Surface elemental analysis of cut PAC particles with adsorbed HOI (A1–A4) and adsorbed organic-I (B1–B4) by means of field emission electron probe microanalysis (FE-EPMA). Initial I^- concentration in sample water, 10,000 µg-I/L; initial DOC concentrations, 0 mg-C/L for panels A1–A4 and 1.5 mg-C/L for panels B1–B4. After chlorination for 10 min at 5 mg-Cl_2/L, PAC was added. After a carbon contact time of 30 min, PAC particles were removed and cut with a focused ion beam.
(A1) Scanning electron micrograph of a cut PAC particle, (A2) elemental mapping of carbon (C) (526–7892 cps), (A3) elemental mapping of iodine (I) (0–323 cps), and (A4) elemental mapping of iodine (I) (125–285 cps). (B1) Scanning electron micrograph of a cut PAC particle, (B2) elemental mapping of carbon (C) (716–10745 cps), (B3) elemental mapping of iodine (I) (0–220 cps), (B4) elemental mapping of iodine (I) (100–200 cps).